

Development of an energy barrier at the metal-chain–metallic-carbon-nanotube nanocontact

Kijeong Kong, Seungwu Han, and Jisoon Ihm

Department of Physics and Center for Theoretical Physics, Seoul National University, Seoul 151-742, Korea

(Received 14 December 1998; revised manuscript received 9 April 1999)

We perform *ab initio* pseudopotential calculations for a nanocontact between a metallic carbon nanotube and a copper chain. We find that the on-top position is the most stable geometry of the copper chain on the nanotube and a local energy gap of ≈ 0.1 eV opens as the mirror symmetry of the nanotube is broken by the presence of copper. A weak ionic bonding is formed between the tube and the copper chain and the charge density in the conducting channel around the Fermi level is reduced at the contact region. Therefore, the electronic transport across the contact occurs essentially through the tunneling process. Appearance of such a locally semiconducting property in the intrinsically metallic carbon nanotube may explain the unusual low-temperature current-voltage characteristics exhibiting a huge contact resistance or a quantum dot behavior. [S0163-1829(99)05831-2]

I. INTRODUCTION

Due to the quasi-one-dimensional geometry and various electronic properties, the carbon nanotube¹ (CNT) is thought to be a good candidate for a building block of new nano-sized electronic devices, possibly overcoming the limit of the current silicon-based technology. It is well known that, although built only of carbon atoms, the CNT can be a metal or a semiconductor depending on its chirality and radius,²⁻⁵ and among them the so-called (n,n) -type tubes⁴ are metallic with the resistivity down to $\sim 10^{-5}$ Ω cm, almost comparable to that of typical metals.^{6,7}

There have been many experiments reporting current-voltage (I - V) characteristics of ropes⁸ and metallic single-wall tubes^{9,10} at low temperature. In these experiments, it is found that the low-temperature conductance is dominated by the single-electron transport; the conductance as a function of the gate voltage consists of a series of sharp peaks separated more or less evenly by regions of very low conductance, a characteristic of a quantum dot. Since the quantum dot behavior is expected only for an “island” almost isolated from metallic probes that measure the conductance, the result implies that there may exist a small but finite energy barrier between the metallic lead and the CNT. Although these experiments alone do not “prove” the existence of the barrier, another experimental observation that the resistance across the junction between an ordinary metal probe and a metallic tube is indeed very high also suggests such a possibility. For example, multiprobe experiments with Pt leads are reported to have a high electrode-CNT contact resistance (1–4 M Ω).^{9,10} For a typical metal-metal nanocontact, the resistance would be of the order of the (spin-degenerate) quantum resistance $R_c = h/2e^2 \sim 13$ k Ω . Since the π bonding state of the conducting electrons in the CNT is quite different from the free-electron-like state in a typical metal, the contact between the metallic tube and the ordinary metal may conceivably show different behaviors from a typical metal-metal junction.

Even though the intrinsic transport property of the CNT has been under extensive study, its contact with other metal-

lic systems has not been well investigated on the level of *ab initio* calculations to our knowledge. In this paper, we consider a model system which consists of a metallic tube in contact with a copper chain lying perpendicular to it. It is not possible yet to consider a bulk metallic wire or a metal substrate because of the computational limitation on the unit supercell size. Although a chain seems to be a somewhat artificial model for a real wire, there is a justification for using a chain. In usual experiments, two bulk metallic wires are deposited first and a CNT is laid across them. Owing to the finite modulus of the tube against bending, the contact between the metallic wire and the tube is most likely to be a linear chain as depicted in Fig. 1. A computational complication may arise because the tube is actually bent at the contact, but we are justified to study the straight tube since the bending of the tube has been shown to have a negligible effect on the electronic structure around the Fermi level.¹¹ (Buckling is not considered here.) We choose Cu for a metallic probe material because of our previous experience and familiarity with the pseudopotential calculation of Cu.¹² We will show below, by means of the *ab initio* pseudopotential calculations, that a local energy gap develops at the contact which gives rise to a large contact resistance. We will also demonstrate that a weak ionic bonding is formed between the tube and the copper chain, resulting in a reduction of the charge at the contact region for the states near the Fermi level and a further increase of the contact resistance.

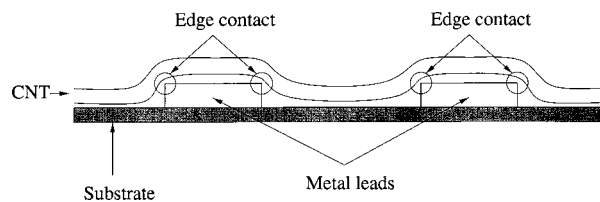


FIG. 1. Cross section of a typical experimental setup measuring current-voltage characteristics. Due to the finite binding energy with the substrate, the CNT tends to distort to conform to the substrate topography. The metal edge in the contact region can be approximated as a metal chain.

II. COMPUTATIONAL SETTING AND EQUILIBRIUM GEOMETRIES

We carry out conventional *ab initio* pseudopotential calculations within the local density approximation (LDA) using the plane-wave basis set.¹³ We generate a semilocal pseudopotential following the scheme of Troullier and Martins¹⁴ and make it fully nonlocal according to the Kleinman and Bylander procedure.¹⁵ The calculations are performed for an orthorhombic supercell with the closest distance between atoms on different tubes larger than 6 Å, which keeps the undesirable tube-tube interaction sufficiently small. In order to reduce the computational load, we use a rather small (5,5) metallic nanotube with a diameter of about 6.7 Å, which corresponds to perhaps the smallest CNT so far synthesized. Metal chains are separated by three CNT unit cells (7.5 Å) along the direction of the nanotube axis in our supercell geometry. The energy cutoff is 50 Ry and a large number of plane waves ($\sim 450\,000$) are used for this calculation. The Brillouin zone integration is done with three \mathbf{k} points in the irreducible Brillouin zone for the potential convergence and with 24 \mathbf{k} points for the calculation of the density of states. The density of states is approximated using a Gaussian broadening of 0.01 eV. For the geometry optimization, we employ both the energy minimization technique and the molecular dynamics. Coordinates of the carbon atoms of the CNT are relaxed using Hellmann-Feynman forces and quantum mechanical stresses. The C-C distance in the circumferential direction is 1.41 Å and the periodicity in the axis direction is 2.5 Å, both within 2% deviation from the dimensions of the ideal graphene sheet. The effect of this small relaxation on the electronic band structure is negligible.¹⁶ We use a linear copper chain for representing a metal probe contacting the CNT as mentioned in the Introduction. The optimized interatomic distance in the isolated Cu chain is 2.49 Å and the cohesive energy is 1.72 eV per atom.

We have investigated three geometries of the Cu-chain-CNT complexes. They are on-top, bridge, and center geometries, and we have confirmed that each of them is a local energy minimum by examining the Hellmann-Feynman forces of slightly shifted geometries. The respective geometries of the isolated Cu chain and the isolated CNT are kept the same as determined above and only the distance between them is allowed to vary. These geometries are visualized in Fig. 2. The tubule axis lies in the x direction and the metal chain is in the z direction. In the following, the Cu-chain-carbon-nanotube complex shall be abbreviated as the Cu-CNT.

In the on-top geometry, the Cu atom nearest to the CNT is located right above a C atom and the equilibrium distance between them is 2.06 Å. We denote the nearest-neighbor copper atom to the CNT as Cu1 and the next nearest neighbor as Cu2 as shown in the figure. In the bridge geometry, the Cu atom nearest to the tube is located right above the center of the C-C bond of the CNT and the nearest-neighbor distance between C and Cu is 2.36 Å. The weakest Cu-C bond forms in the center geometry, where the Cu atom is right above the center of a hexagonal ring of carbons and the equilibrium distance is 2.42 Å. The equilibrium distance and the heat of formation of each geometry are summarized in

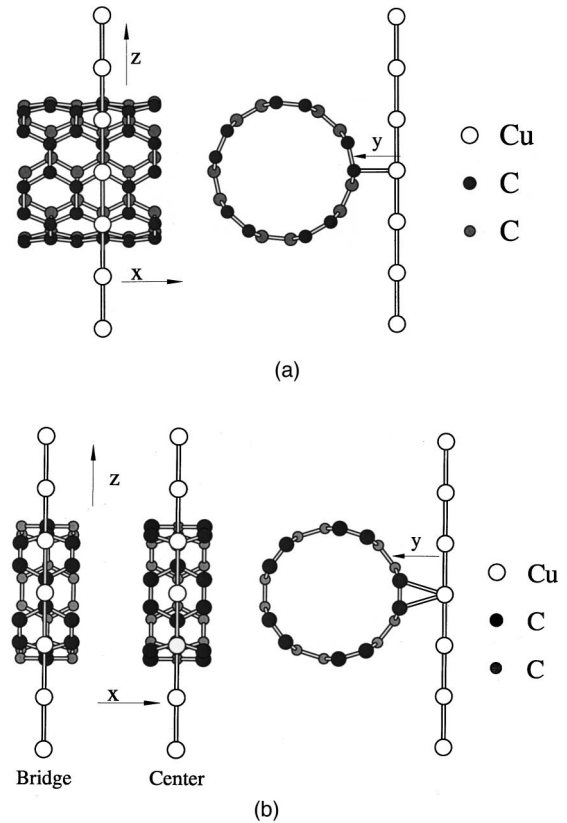


FIG. 2. Model geometries of the Cu-CNT. The tubular axis lies in the x direction and the Cu chain lies in the z direction. The side view and the cross section of the tube containing the chain are shown for (a) the on-top geometry and (b) the bridge and the center geometries. For visual clarity, half of the carbon atoms are denoted by smaller and gray filled circles.

Table I. The heat of formation H_f is obtained by subtracting the total energy of the Cu-CNT from the sum of the total energies of the isolated Cu chain and the CNT. The on-top geometry is the most stable, and the energy difference between the on-top and other geometries is 1.5–2 eV. The dipole moment of each geometry is calculated and its component along the contact (y) direction is given. Detailed discussions about the dipole moment and its derivative with respect to the bond length (equal to dynamic charge) will be given later.

Another *ab initio* calculation in the literature on the adsorption of the transition metal atoms on the CNT edge shows a similar difference in the equilibrium distance (about ~ 0.46 Å) between the on-top and the center sites.¹⁷ This is

TABLE I. Calculated properties of the Cu-CNT complexes with different copper positions with respect to the CNT. d_{NN} is the equilibrium distance between the nearest-neighbor Cu and C atom, H_f is the heat of formation, μ_y is the y component of the dipole moment, and q_d ($= \partial\mu/\partial d$) is the dynamical charge.

Geometry	d_{NN} (Å)	H_f (eV)	μ_y (D)	q_d (e)
Atop	2.06	3.05	3.5	3.9
Bridge	2.36	1.58	-2.4	0.2
Center	2.42	0.97	-2.9	0.1

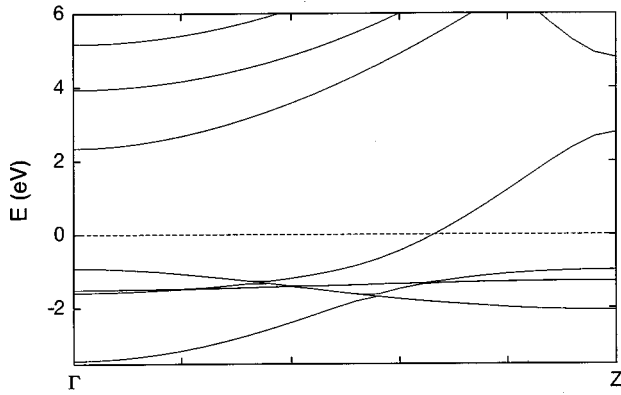


FIG. 3. One-dimensional band structure of the Cu chain with the equilibrium interatomic distance. The Fermi level is set to zero.

well explained by Pauling's theory that a less coordinated atom exhibits a shorter bond length and a stronger bonding. Only one bond is formed between the nearest-neighbor C and the Cu1 in the on-top geometry whereas the number of Cu-C nearest neighbors is 6 in the center geometry. The case of the center geometry is comparable to the potassium atom inserted at the center of the $(n,0)$ carbon nanotube where the maximum H_f is about 1 eV.¹⁸ The binding energy of the tube to the passivated silicon surface is reported to be 0.8 ± 0.3 eV/Å,¹⁹ but a direct comparison with the present case is inappropriate because the bonding in Ref. 19 is obviously of the van der Waals type.

III. BAND STRUCTURE

The one-dimensional band structure for the isolated Cu chain is shown in Fig. 3. At Γ , the highest occupied molecular orbital (HOMO) is doubly degenerate $3d$ states and the energy of the $4s$ -derived state is slightly lower. The $3d$ band crosses the $4s$ band at the wave vector of $\sim 34\%$ toward the X point and thereafter the $4s$ band is the HOMO. Since copper has 11 valence electrons, the HOMO is half filled and the Fermi energy crosses the $4s$ band. In the bulk copper, conduction occurs only through the $4s$ band. In the Cu-chain case, the nondegenerate $4s$ band and some degenerate $3d$ bands are clustered around the Fermi level and the conducting behavior is more complex than in the bulk case. In fact we will show below that the $3d$ electrons play a crucial role in the electronic transport across the junction.

Figure 4 shows band structures of the Cu-CNT along the chain (z) and the nanotube axis (x) direction in the on-top and the bridge geometries. Since the Cu chain lies in the z direction, Cu-derived bands are flat along the x direction and likewise the CNT-derived bands are flat along the z direction. The $4s$ band of the Cu chain mixes strongly with the π^* band of the CNT around the Γ point. In the real space picture, the metallic tube becomes locally semiconductive around the contact region in the on-top geometry by the perturbation from the Cu chain. Existence of the copper chain breaks the mirror symmetry of the CNT and lifts the degeneracy of the π^* and the π bands.²⁰ In Fig. 4(a), the band gap along Γ - X is about 0.08 eV. This gap opening is not found in other geometries where the mirror symmetry is maintained in spite of the existence of the copper chain. In the on-top ge-

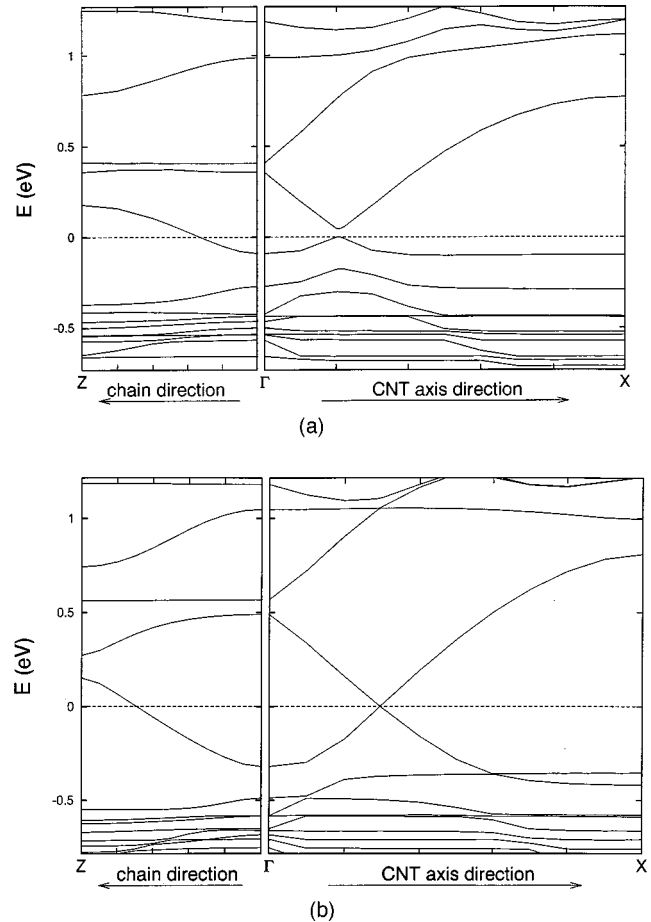
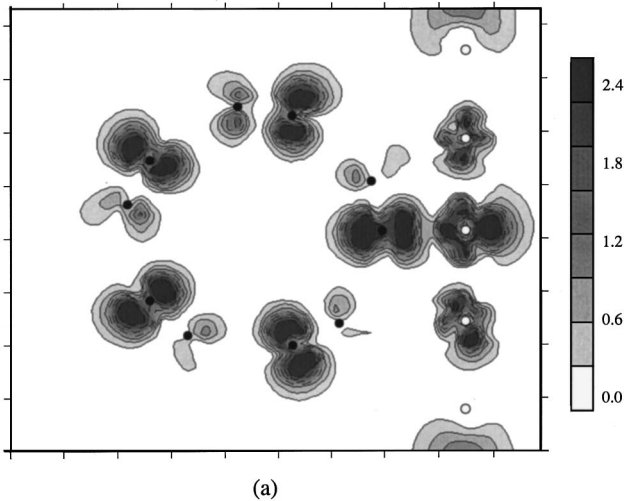


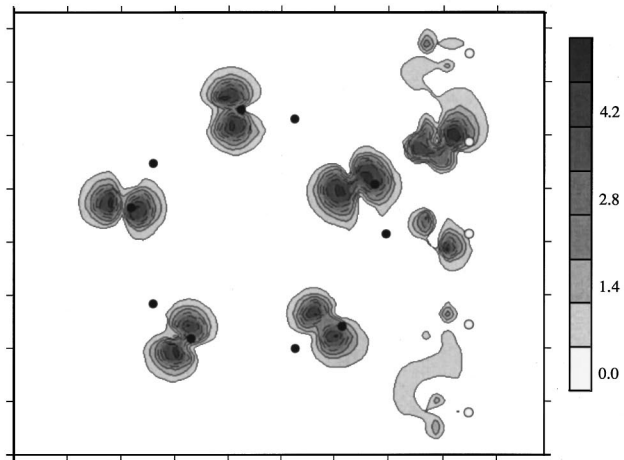
FIG. 4. Band structure of the Cu-CNT in (a) the on-top and (b) the bridge geometries.

ometry, the Fermi level lies in this band gap for $k_z=0$, but it crosses the dispersive copper band for a finite k_z (which must be the case since copper is a metal, anyway).

Opening of a small band gap partially explains the large contact resistance observed in experiment. The contact between a metallic tube and an ordinary metal electrode resembles a semiconductor-metal (Schottky-type) rather than a metal-metal junction. The metallic character of the (n,n) nanotube is quite fragile, unlike in other typical metals, because two bands cross exactly at the Fermi level and the crossing is easily lifted by a small symmetry-breaking perturbation.²⁰ In Fig. 5, we present the charge density of the HOMO and lowest unoccupied molecular orbital (LUMO) at the gap opening \mathbf{k} point in the yz plane containing the contact point. We find that the breakup of the π - π^* degeneracy is accompanied by an appearance of a spatial charge modulation with a two-atom period. In an isolated CNT, the electronic charge for the degenerate states at the band crossing point is equally distributed over all carbon atoms. In our model system, on the other hand, the Cu chain is in close contact with one particular carbon atom. Among two states split by the perturbation from Cu, one, say, $(1/\sqrt{2})(|\pi\rangle + |\pi^*\rangle)$, is localized predominantly at one of the two hexagonal sublattices thereby exhibiting the charge modulation of the two-atom period. The other partner, $(1/\sqrt{2})(|\pi\rangle - |\pi^*\rangle)$, is localized at the other sublattice. Since the bonding interaction between the nearest-neighbor C and Cu low-



(a)



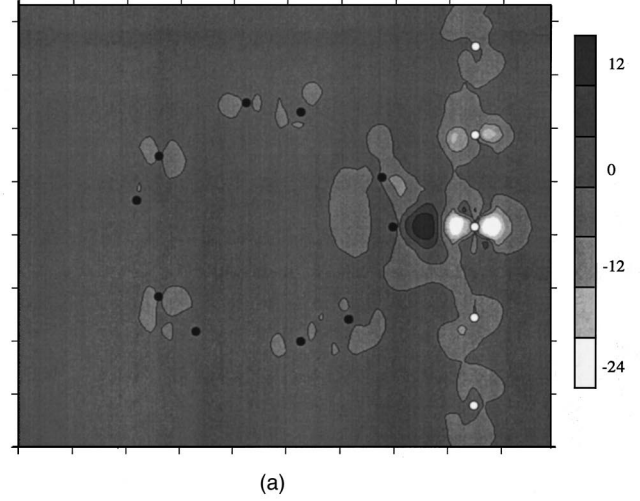
(b)

FIG. 5. Charge density of (a) the HOMO and (b) the LUMO at the gap-opening \mathbf{k} point in the on-top geometry showing the spatial charge modulation with the two-atom period. The open circles correspond to the positions of copper atoms and the filled circles are carbon atoms. The unit is 10^{-3} electron/supercell.

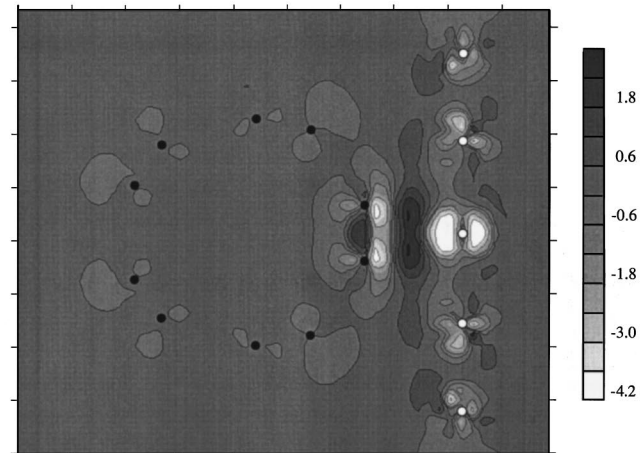
ers the energy level, the state in Fig. 5(a) with such a bonding is the HOMO and the one in Fig. 5(b) is the LUMO.

IV. CHARGE TRANSFER

Now we describe the charge transfer we have found through the self-consistent *ab initio* calculations. We calculate the difference between the charge density of the Cu-CNT and the sum of the Cu chain and the CNT. The density difference is shown in Fig. 6 in the plane perpendicular to the CNT axis containing the contact. In Fig. 6(a) of the on-top geometry, it is obvious that the charge is depleted mainly from Cu1 and Cu2. The depleted charge moves to the CNT surface. The excess charge shows the p_y character (i.e., the π electron) of the contact C atom. Thus the bonding character of the on-top geometry may be regarded as ionic. In the bridge geometry in Fig. 6(b), on the other hand, both the copper chain and the CNT lose their charge which is accumulated in the middle of the junction. Its magnitude is much smaller than the on-top geometry, though. In this geometry,



(a)



(b)

FIG. 6. Charge density difference between the Cu-CNT and the sum of the isolated Cu chain and the CNT in the yz plane crossing the contact in (a) the on-top and (b) the bridge geometries. The open circles indicate the positions of copper atoms and the filled circles are carbon atoms. The charge is accumulated near the carbon atom in the on-top geometry, showing an ionic bonding character whereas the bonding is covalent, though much weaker in strength, in the bridge geometry. The unit is 10^{-3} electron/supercell.

the bonding character is weakly covalent. The density difference plots in both geometries show that the depleted charge from the copper chain has a $3d$ character. The interaction between the CNT and the metal chain is such that not only the $4s$ electron but also the $3d$ electrons in the Cu chain are affected. In the atomic calculation, the energy level of $3d$ electrons is only 0.8 eV lower than that of the $4s$ electron and the energy difference is even smaller in the chain case.

Since materials with ionic bonding are usually insulators, it is conceivable that the ionic bonding we identify here may contribute to further reduction in conductance in addition to the gap opening by the broken symmetry. To see the effect more closely, we integrate the charge density of the states in the energy window from 0.3 eV below up to the Fermi level and plotted it in Fig. 7. Charge is absent at the center of the contact in this important energy range, which means that the conduction of electrons across the metal-CNT junction oc-

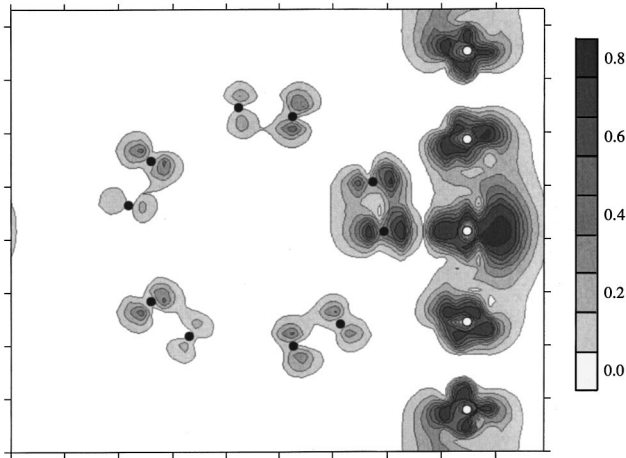


FIG. 7. Integrated charge density over the energy window from 0.3 eV below up to the Fermi level. The open circles indicate the positions of copper atoms and the filled circles are carbon atoms. In this energy range which is crucial to conduction, the charge is depleted from the contact region. The unit is 0.1 electron/supercell.

curs basically through the tunneling process. The present situation is quite different from ordinary metal-metal junctions where conduction occurs rather smoothly via metallic bonds across the junction. The energy of the charge transferred from the Cu 3d bands is well below (around 2 eV below) the Fermi level and it does not contribute to conducting channels under usual bias conditions. Instead, it behaves as a repulsive center pushing away electrons of higher energy, so that the charge density of the conducting electrons near the Fermi level is reduced at the center of the contact. Together with the aforementioned local gap of ≤ 0.1 eV, the charge depletion is expected to reduce the transmission probability of electrons to order of 1% of the perfect channel at low temperature. If there are two channels ($R=6.5$ k Ω) through the Cu-CNT, the resulting resistance is order of 1 M Ω , in rough agreement with experiment.

We also study the local density of states (LDOS) around $x=0$. Both the partial (symmetry-decomposed) and the total LDOS are presented in Fig. 8. Comparing the LDOS of Cu1 with that of the third neighbor Cu atom (denoted by Cu3) in Fig. 8(a), we notice that the 3d electrons in the energy range between -1.5 and -0.5 eV are depleted in the Cu1 atom. In Fig. 8(b), on the other hand, we see that the LDOS around the Fermi level increases at the contact carbon atom (C1) compared with the carbon atom farthest from the Cu chain (C_f), which implies the electrons are transferred from the Cu chain to the CNT.

The amount of the transferred charge estimated by integrating the charge difference is $0.69e$. To confirm this value, we have calculated the y component of the dipole moment and obtained 3.46 Debye as presented in Table I. If we assume that the negative charge is located at the center of the accumulated charge and the positive charge is at the position of Cu1, the distance is ~ 1.38 Å and the charge transfer is $0.52e$, in fair agreement with that mentioned above. We also examine the variation of the dipole moment as a function of the distance between the chain and the CNT. This is known as a dynamical charge²¹ and we get a nonzero value of approximately $3.9e$ in the on-top geometry, which indicates

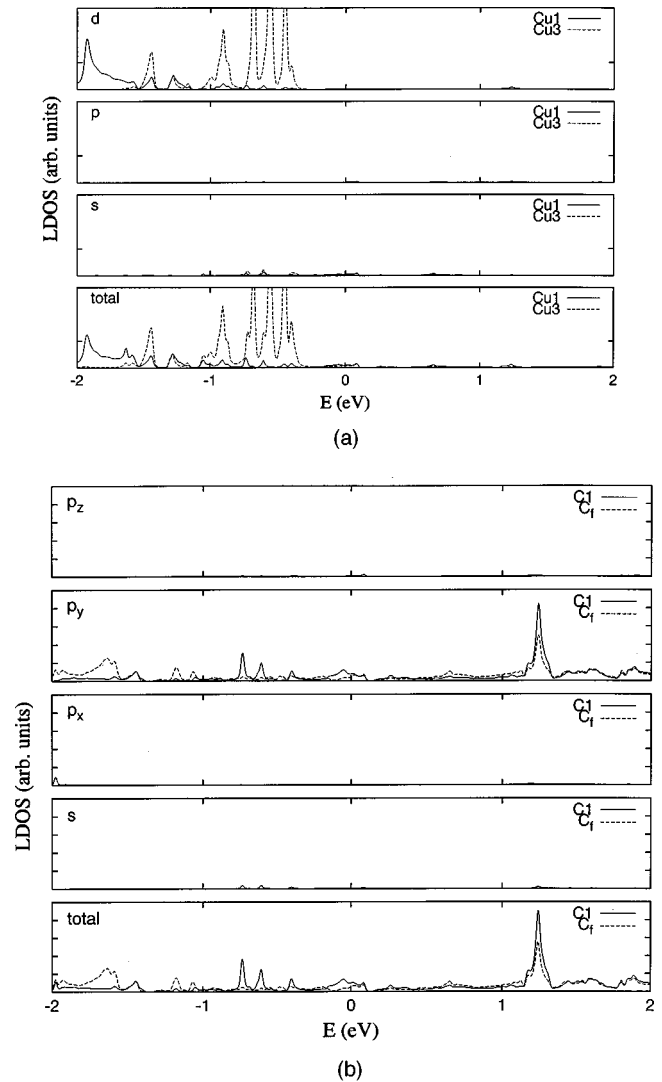


FIG. 8. LDOS of Cu and C atoms. Both the partial (symmetry-decomposed) and the total LDOS are presented. (a) LDOS of Cu atoms; Cu1 is the one in contact with the CNT and Cu3 is the third neighbor. (b) LDOS of C atoms; C1 is the one in contact with Cu and C_f is the farthest one (with the identical y coordinate) from Cu.

that the bonding is ionic. This value of the dynamical charge is much larger than other known cases, e.g., adsorption of Na on the Al surface ($\sim 0.4e$) or Cl on the Al surface ($\sim -0.5e$).²² In the bridge or the center geometry, the dynamical charge is almost zero, indicating a (weakly) covalent bonding character.

We note that there is an experimental report²³ on the charge transfer as well as the energy gap for the tube on the gold substrate, but details seem different from ours. In our system, the mirror symmetry breaking introduces the local gap and the ionic bonding induces the charge transfer. In Ref. 23, on the other hand, the large contact area of the gold substrate causes very little symmetry breaking and the gap presumably originates from the capacitive effect (the Coulomb blockade) and the kinetic energy quantization of the finite-length tube. The charge transfer in Ref. 23 is evidently driven by the matching of the chemical potential of the tube and the gold substrate, and may not be assigned to a particular bond.

V. SUMMARY

We have investigated the atomic and the electronic structure at the contact between the copper chain and the metallic tube using the *ab initio* pseudopotential LDA method. We have examined three geometries of the Cu-CNT and found that the on-top position is the most stable with the energy gain of 1.5–2 eV relative to the bridge or the center position. We have also shown that the bonding character of the Cu-CNT is ionic in the on-top geometry where the charge is transferred to the contact CNT surface from the neighboring Cu atoms. Depletion of the charge in the Cu chain occurs in the low-lying $3d$ bands. The on-top geometry shows a local gap of ~ 0.1 eV around the contact region of the nanotube. As the π - π^* degeneracy is lifted, charge modulation states of the two-atom period appear. Occupation of one of these states breaks the symmetry of the total charge distribution. States near the Fermi level show charge depletion at the center of the contact region, barring the metallic transport of the electrons. This suggests that the conduction occurs via the tunneling process and the region of the nanotube in between

two metal-CNT junctions may be regarded as a quantum dot. It is premature to calculate the conductance of our geometry and compare it directly with experiment because our model is a rather simplified one. Still, our result seems to agree at least qualitatively with many experiments reporting either a contact resistance of ~ 1 M Ω or a basically semiconductive behavior of the junction. Furthermore, since we have identified at least some of the origins of the large contact resistance, it seems possible that, by optimizing the contact geometry in a realistic junction of the tube with a bulk metallic wire, the symmetry-breaking gap and the charge transfer may be minimized and the contact resistance may be significantly reduced.

ACKNOWLEDGMENTS

This work was supported by the International Cooperative Program of the Korea Science and Engineering Foundation, the BSRI of the Ministry of Education, and the SRC program of the CTP. The computation was done using the supercomputer at the Supercomputing Center at ETRI.

-
- ¹S. Iijima, *Nature (London)* **354**, 56 (1991).
²R. Saito, M. Fujita, G. Dresselhaus, and M. S. Dresselhaus, *Appl. Phys. Lett.* **60**, 2204 (1992).
³N. Hamada, S. Sawada, and A. Oshiyama, *Phys. Rev. Lett.* **68**, 1579 (1992).
⁴D. H. Robertson, D. W. Brenner, and J. W. Mintmire, *Phys. Rev. B* **45**, 12 592 (1992).
⁵J. W. Mintmire, B. I. Dunlap, and C. T. White, *Phys. Rev. Lett.* **68**, 631 (1992).
⁶A. Y. Kasumov, I. I. Khodos, P. M. Ajayan, and C. Colliex, *Europhys. Lett.* **34**, 429 (1996).
⁷T. W. Ebbesen, H. J. Lezec, H. Hiura, J. W. Bennett, H. F. Ghaemi, and T. Thio, *Nature (London)* **382**, 54 (1996).
⁸M. Bockrath, D. H. Cobden, P. L. McEuen, N. G. Chopra, A. Zettl, A. Thess, and R. E. Smalley, *Science* **275**, 1922 (1997).
⁹S. J. Tans, M. H. Devoret, H. Dai, A. Thess, R. E. Smalley, L. J. Geerligs, and C. Dekker, *Nature (London)* **386**, 474 (1997).
¹⁰A. Bezryadin, A. R. M. Verschueren, S. J. Tans, and C. Dekker, *Phys. Rev. Lett.* **80**, 4036 (1998).
¹¹C. L. Kane and E. J. Mele, *Phys. Rev. Lett.* **78**, 1932 (1997).
¹²We have recently confirmed that the calculational results with the Au chain are identical.
¹³J. Ihm, A. Zunger, and M. L. Cohen, *J. Phys. C* **12**, 4409 (1979).
¹⁴N. Troullier and J. L. Martins, *Phys. Rev. B* **43**, 1993 (1991).
¹⁵L. Kleinman and D. M. Bylander, *Phys. Rev. Lett.* **48**, 1425 (1982).
¹⁶X. Blase, L. X. Benedict, E. L. Shirley, and S. G. Louie, *Phys. Rev. Lett.* **72**, 1878 (1994).
¹⁷Y. H. Lee, S. G. Kim, and D. Tomanek, *Phys. Rev. Lett.* **78**, 2393 (1997).
¹⁸Y. Miyamoto, A. Rubio, X. Blase, M. L. Cohen, and S. G. Louie, *Phys. Rev. Lett.* **74**, 2993 (1995); A. Rubio, Y. Miyamoto, X. Blase, M. L. Cohen, and S. G. Louie, *Phys. Rev. B* **53**, 4023 (1996).
¹⁹T. Hertel, R. Martel, and P. Avouris, *J. Phys. Chem. B* **102**, 910 (1998).
²⁰P. Delaney, H. J. Choi, J. Ihm, S. G. Louie, and M. L. Cohen, *Nature (London)* **391**, 466 (1998).
²¹N. D. Lang and A. R. Williams, *Phys. Rev. B* **18**, 616 (1978).
²²J. Bormet, J. Neugebauer, and M. Scheffler, *Phys. Rev. B* **49**, 17 242 (1994).
²³L. C. Venema, J. W. G. Wildöer, J. W. Janssen, S. J. Tans, H. L. J. Temminck Tuinstra, L. P. Kouwenhoven, and C. Dekker, *Science* **283**, 52 (1999).